Toward Assessment of Density Functionals for Vibronic Coupling in Two-Photon Absorption: A Case Study of 4-Nitroaniline

Robert Zaleśny,*[a,b] Guangjun Tian,[b] Christof Hättig,[c] Wojciech Bartkowiak,[a] and Hans Ågren*[b]

In this study, we predict vibronic two-photon absorption (TPA) spectra for 4-nitroaniline *in vacuo*. The simulations are performed using density functional theory and the approximate second-order coupled-cluster singles and doubles model CC2. Thereby we also demonstrate the possibility of simulations of vibronic TPA spectra with *ab initio* wavefunction methods that include electron correlation for medium-sized systems. A special focus is put on the geometric derivatives of the second-order transition moment and the dipole moment difference between the charge-transfer excited state and the ground state. The results of CC2 calculations bring new insight into the vibronic coupling mechanism in TPA spectra of 4-nitroniline and demonstrate that the mixed term is quite large and that it also exhibits a negative interference with the Franck-Condon contribution. © 2015 Wiley Periodicals, Inc.

DOI: 10.1002/jcc.23903

Introduction

As the seminal papers of Champagne and coworkers,[1–3] who demonstrated the limited applicability of most conventional functionals in the field of molecular nonlinear optics, several other research groups have aimed at the assessment of exchange-correlation functionals in predicting purely electronic resonant and nonresonant (hyper)polarizabilities.[4,5] Some new functionals were proposed, based on the idea of splitting of electron repulsion operator into short-range and long-range parts. These functionals are referred to as long-range corrected or range-separated functionals and are usually abbreviated as LC-DFT, LR-DFT, or LRC-DFT. A broad range of chemical systems has been studied with the aim to analyze the performance of density functional theory (DFT) and LC-DFT, covering small to relatively large molecules. Hammond and Kowalski used four functionals (PBE, PBE0, B3LYP, and CAM-B3LYP) to study the dipole hyperpolarizability of two small molecules (CH_3CN, $CHCl_3$) and 4-nitroaniline.[4] These authors reported that the CAM-B3LYP functional is generally superior to conventional GGA and GGA-hybrid functionals for small molecules but for 4-nitroaniline it does not deliver more accurate results than the other used functionals. A performance analysis of LC-DFT in predicting electric-dipole hyperpolarizabities for an extensive set encompassing 59 organic molecules in solution has recently been reported by Lu,[6] who concluded that range-separated hybrids deliver more accurate estimates of the properties in question than global hybrids. These conclusions confirm earlier findings for 82 organic molecules reported by the same research group.[7] Baranowska-Łączkowska et al. investigated several medium-sized organic π-conjugated molecules in the gas-phase and demonstrated that, on average, LC functionals improve the predictions of first and second hyperpolarizabilities relative to global hybrid functionals.[8] Some of the molecules studied by Baranowska-Łączkowska appeared to be very problematic even for LC-DFT.[8] Likewise, Jacquemin et al. reported that short polymethineimine oligomers are challenging for LC-DFT.[9] A possibility to overcome these difficulties might be a further reparametrization of the range-separation parameter (μ). In fact, such a route has been recently followed by Nénon et al.[10] These authors made an attempt to analyze the performance of long-range corrected functionals with a physically adjusted range-separated parameter for computing the polarizability and the second hyperpolarizability of π-conjugated oligomers of increasing size (i.e., polydiacetylene and polybutatriene chains). The primary conclusion that emerged from the latter study is that an adjustment of μ offers no advantage over traditional values ($\mu = 0.33$ or 0.47).[10] These conclusions are in line with what has been reported recently by Garrett et al. for the first hyperpolarizability of 14 organic chromophores.[11] LC-DFT is also a common choice for studies of

[a] *R. Zaleśny, W. Bartkowiak*
Department of Physical and Quantum Chemistry, Faculty of Chemistry, Wrocław University of Technology, Wyb. Wyspiańskiego 27, PL-50370 Wrocław, Poland
E-mail: robert.zalesny@pwr.edu.pl

[b] *R. Zaleśny, G. Tian, H. Ågren*
Division of Theoretical Chemistry and Biology, School of Biotechnology, Royal Institute of Technology, SE-10691 Stockholm, Sweden
E-mail: hagren@kth.se

[c] *C. Hättig*
Lehrstuhl fuer Theoretische Chemie, Ruhr-Universität Bochum, Universitätsstrasse 150, D-44780 Bochum, Germany

Contract grant sponsor: Swedish Infrastructure Committee for the project "Multiphysics Modeling of Molecular Materials" (Computer resources); Contract grant number: SNIC 025/12–38; Contract grant sponsor: National Science Centre; Contract grant number: DEC-2011/01/D/ST4/03149

© 2015 Wiley Periodicals, Inc.

resonant nonlinear optical properties, as for instance two-photon absorption (TPA).[12–15] In particular, it has been observed that CAM-B3LYP delivers satisfactory estimates of TPA cross sections (σ^{2PA}) for organic molecules in solution.[16,17]

As briefly summarized in the preceding paragraph, there are many benchmarks of (LC)-DFT for electronic hyperpolarizabilities. However, not much is known about the performance of density functionals in computing geometrical derivatives of high-order electric-dipole properties. Derivatives of the electronic dipole moment and the polarizability with respect to normal modes are necessary to determine infrared and Raman intensities in vibrational spectroscopy. Geometric derivatives of higher-order electric properties are necessary to determine vibrational contributions to static and dynamic vibrational hyperpolarizabilities. For instance, the determination of the nuclear relaxation contribution to electric field-induced second harmonic generation (ESHG) requires (within the infinite optical frequency approximation) derivatives of the first hyperpolarizability with respect to the normal modes. It is somewhat unfortunate that the assessment of exchange-correlation functionals has been scarcely performed for such derivatives. In a series of papers, some of the present authors contributed to this subject by analyzing the predictive power of (LC)-DFT in computing static vibrational hyperpolarizabilities, including anharmonic contributions.[18,19] It has been demonstrated for a series of polymethineimine oligomers that the CAM-B3LYP functional yields the best overall results in the case of nonresonant vibrational hyperpolarizabilities. For some nonlinear optical processes, like for instance ESHG, none of the studied functionals predicts the correct sign of the vibrational contribution for polymethineimine oligomers.[19] However, it has been shown for donor–acceptor-substituted azobenzenes that in the case of vibrational contributions to ESHG the CAM-B3LYP functional outperforms the B3LYP functional and yields results much closer to the MP2 reference.[18] In the present study, we aim at extending our previous efforts regarding nonresonant vibrational hyperpolarizabilities and perform an assessment of density functionals for resonant nonlinear optical properties. Our focus is on the geometric derivatives of two-photon transition moments (M, see next section for its definition). This quantity appears in various models for vibronic coupling in TPA.[13],[20–23] In their recent study, Drobizhev et al. studied the vibronic coupling mechanism in TPA spectra of fluorescent proteins.[24] The key parameter in the model proposed by these authors is the geometric derivative of the dipole moment difference ($\Delta\mu$) between an excited state and the ground state. The approximate representation of the two-photon transition moment by $\Delta\mu$ proved to be successful in interpreting experimental data.[24] We thus include the geometric derivatives of $\Delta\mu$ in the present study. It is fair to mention that the most rigorous treatment of vibrational contributions to TPA is that by Bishop et al.[22] These authors demonstrated, based on double perturbation theory, how to include the electrical and mechanical anharmonicity through second order in perturbation theory. The method of Bishop et al. has, however, only been applied to carbon monoxide. More approximate treatments rely on the lowest-order terms in the Herzberg–Teller expansion of the second-order transition moment with respect to the normal coordinates. A model that falls into this rubric is known as the linear coupling model and has been successfully used to simulate the vibrational fine structure of TPA bands in spectra of medium-sized molecules.[25] This model retains terms up to linear order in the normal coordinates.

A thorough analysis of the physical grounds of the models used to analyze vibronic coupling in TPA spectra would go beyond the scope of the present study. We exclusively focus on: (i) analysis of vibrational fine structure of band corresponding to two-photon $\pi \rightarrow \pi^{\star}$ transition in the spectra of 4-nitroaniline, (ii) comparative assessment of exchange-correlation functionals in the prediction of vibronic two-photon spectrum, $\partial M^{XY}_{0\leftarrow J}/\partial Q_k$ and $\partial(\Delta\mu)/\partial Q_k$ for the normal coordinates Q_k. For this we use a new implementation[14] of the CC2 method[26] for TPA to determine reference values for 4-nitroaniline *in vacuo*. The molecule in question is a prototypical donor-π-acceptor system which possesses a low-lying intramolecular charge transfer state and it is thus a well-suited testbed for the assessment of density functionals.

Computational Methods

The two key quantities, which are the subject of the present study, are (i) geometric derivatives of two-photon transition moments ($\partial M^{XY}/\partial Q_k$, where Q_k denotes the kth normal coordinate of vibration) and (ii) geometric derivative of the dipole moment difference between an excited state and the ground state ($\partial(\Delta\mu)/\partial Q_k$), evaluated at the equilibrium geometry of the latter. The two-photon transition moments between the ground state $\langle 0|$ and an excited state $\langle J|$ is defined as:[27,28]

$$M^{XY}_{0\leftarrow J} = \hat{P}^{XY} \sum_K \frac{\langle 0|X|K\rangle\langle K|Y|J\rangle}{\omega_X - \omega_K} \tag{1}$$

$$M^{XY}_{J\leftarrow 0} = \hat{P}^{XY} \sum_K \frac{\langle J|X|K\rangle\langle K|Y|0\rangle}{\omega_X - \omega_K} \tag{2}$$

where $\hat{P}^{XY}$ is a permutation operator that exchanges the transition operators X and Y, ω_X and ω_Y denote the corresponding frequencies and K labels excited states. Both $\partial M^{XY}/\partial Q_k$ and $\partial(\Delta\mu)/\partial Q_k$ are evaluated for the transition to the lowest-lying $(\pi, \pi^{\star})$ electronic excited state of 4-nitroaniline which results in an intramolecular charge transfer. For this transition the diagonal component of the two-photon transition moment along the symmetry axis is by far the largest; thus, only geometric derivatives of M^{ZZ} are discussed in this article. In coupled-cluster response theory, unlike in a symmetric configuration interaction like exact-state formulation, $M^{XY}_{0\leftarrow J}$ and $M^{XY}_{J\leftarrow 0}$ are not complex conjugates to each other. This is a result of the biorthogonal similarity-transformed representation of the bra and ket states in coupled-cluster theory.[28] Thus, to make a valid comparison between the DFT and CC2 results, we calculate in the latter case $\sqrt{M^{ZZ}_{0\leftarrow J} M^{ZZ}_{J\leftarrow 0}}$. $\partial M^{ZZ}/\partial Q_k$ and $\partial(\Delta\mu)/\partial Q_k$) derivatives are evaluated numerically by computations of M^{ZZ} and $\Delta\mu$ at a set of displaced geometries followed

by the transformation to the normal coordinate basis. The stability of numerical differentiation was controlled with the aid of the Rutishauser–Romberg algorithm (using the displacements $\pm 2^n h$, where $h = 0.002$ bohr and $n = 0,1,2,3$).[29] To further assess the accuracy of $\partial(\Delta\mu)/\partial Q_i$, the ground-state dipole moment was differentiated with respect to the geometric distortions to yield the infrared intensity. The estimated error with respect to the intensities computed using analytic derivatives was not larger than 0.01 [Debye^2/(Å^{2}amu)]. Note that the same level of theory is used for determining normal coordinates and property derivatives. In this study we also make an attempt to simulate the vibronic TPA spectrum using the linear-coupling model.[21] For this we use Lorentzian broadening to obtain the convoluted spectra. All results reported herein were determined using Dunning's correlation consistent basis sets.[30–32] The set of studied functionals encompasses CAM-B3LYP,[33] B3LYP,[34] BHandHLYP,[35] M06, M06-2X, M06-HF,[36,37] PBE0,[38,39] LC-BLYP,[40] and ωB97X.[41] For computations with the CAM-B3LYP functional we used $\alpha = 0.19$, $\beta = 0.46$, and $\mu = 0.33$, while in the case of the LC-BLYP functional $\mu = 0.47$ was used. Calculations within the density functional theory framework have been performed using the DALTON[42] (M^{ZZ} and its derivatives) and GAUSSIAN 09 suite of programs[35] ($\Delta\mu$ and its derivatives). All CC2 results were obtained adopting the resolution-of-identity (RI) approximation with the aid of a development version of the TURBOMOLE program.[43,44] The details of the RI-CC2 implementation can be found elsewhere.[14,45] For all RI-CC2 calculations we used auxiliary basis sets optimized for the used one-electron basis sets.[46]

Results and Discussion

As pointed out in the preceding sections, vibronic profiles in TPA spectra can be simulated using a Herzberg–Teller expansion of the two-photon transition moment or the dipole moment difference between an excited state and the ground state. The latter approach was used by Rebane et al. to analyze the vibrational fine structure of absorption bands in TPA spectra of fluorescent proteins.[24] In fact, the approximate representation of the two-photon transition moment by the dipole moment difference appears commonly in few-state models used for establishing structure-property relationships for TPA-active materials. The success of such an approximate representation is dependent on the interplay of optical channels that contribute to a two-photon transition. To the best of our knowledge, there is no data available in the literature regarding the performance of quantum chemistry methods in computing geometric derivatives of dipole moment differences on excitation except one study,[47] which indicates that $\Delta\mu$ depends strongly on the exchange-correlation functional. In Table 1 we present the orbital-relaxed ground- and excited-state dipole moments[48,49] of 4-nitroaniline *in vacuo*. The ground state dipole moment is predicted at the density functional level to be between 6.9 and 7.3 D and is almost 1 D larger than the experimental value. We note the satisfactory performance of CC2 for the ground state property. In the excited state, all used exchange-correlation functionals predict the dipole moment to be much smaller than that determined experimentally and the difference is roughly 3 D. The CC2 model is more accurate and the difference is reduced to 1.5 D. Among used functionals, M06-HF delivers the worst predictions of $\Delta\mu$. The results of the performed analysis (see Supporting Information) do not allow to directly link this failure with the amount of Hartree–Fock exchange. The data in Table 1 also demonstrates that the lack of diffuse functions introduces at the CC2 level of theory some error which is not very significant neither in the ground nor in the electronically excited state. To sum up, the applied exchange-correlation functionals overestimate the dipole moment in the ground state and underestimate the dipole moment in the (π,π^*) excited state. However, we note much larger variations in the latter, that is, at the DFT level the standard deviation of the ground and excited state dipole moment is 0.1 D and 0.4 D, respectively. Similar observations have been recently reported by Eriksen et al. who studied ground and excited state dipole moments of 4-nitroaniline in gas-phase and in water. [50] These authors linked the inability of TDDFT/CAM-B3LYP to correctly predict the solvatochromic shift to the underestimated value of the dipole moment difference between the charge-transfer state and the ground state. It should be noted that the CC2 value of $\Delta\mu$ reported herein (7.5 D) is very close to the CCSD result (7.2 D) for 4-nitroaniline in the gas phase reported by Eriksen et al.[50] The conclusion drawn based on the analysis of results for 4-nitroaniline was proved by Bednarska et al. to hold also for another push–pull π-conjugated molecule, that is, 4-nitro-4′-dimethylamino-azobenzene.[47]

Table 1. Ground and vertical (π,π^*) excited-state dipole moments (in Debye) of 4-nitroaniline *in vacuo*.

	μ_g	μ_e	$\Delta\mu$
B3LYP	7.3	12.6	5.3
BHandHLYP	7.1	12.2	5.1
CAM-B3LYP	7.0	12.6	5.6
LC-BLYP	7.0	12.1	5.1
M06	7.1	12.4	5.3
M06-2X	6.9	11.8	4.9
M06-HF	7.0	11.3	4.3
PBE0	7.1	12.6	5.5
CC2	6.3	13.8	7.5
CC2/cc-pVTZ	6.0	13.7	7.7
Expt.	6.2	15.3 ± 1	9.1 ± 1

Unless otherwise indicated, all values (given in [Debye]) were computed using the aug-cc-pVTZ basis set at the equilibrium geometry corresponding to the method indicated below. Experimental value of μ for gas phase was extracted from the measurements in dioxane solution by applying the Onsager reaction field model to eliminate the effect of solvent.[48]

Figure 1 presents the strength of the coupling of the dipole moment difference to the normal modes of vibration in the range of 1100–1800 cm^{-1}. Outside the indicated region the coupling is weak and does not exceed 1 D/(Å$\sqrt{\text{amu}}$). The assignments of some key modes with the largest coupling to $\Delta\mu$ and the corresponding unscaled harmonic vibrational frequencies are given in Table 2. For the sake of brevity, we refer

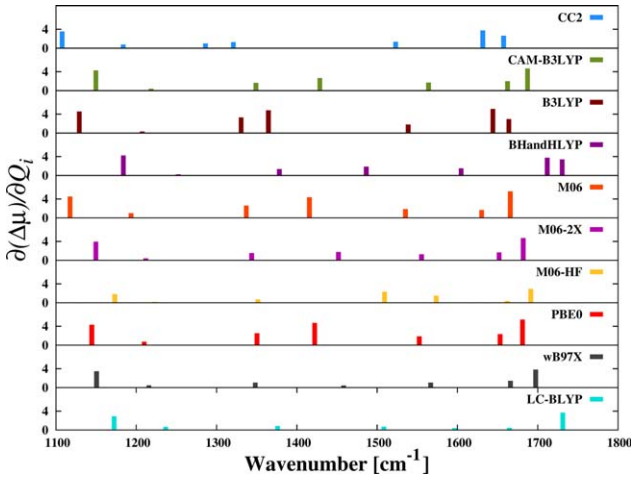


Figure 1. Geometric derivatives of dipole moment difference between the (π,π^*) excited state and the ground electronic state for 4–nitroaniline *in vacuo*. All values are given in [Debye/(Å$\sqrt{\text{amu}}$)] and were calculated using the cc-pVTZ basis set. [Color figure can be viewed in the online issue, which is available at wileyonlinelibrary.com.]

to the five normal modes in question as n_1-n_5. The results presented in Figure 1 and Table 2 were obtained using the cc-pVTZ basis set. Computations of property derivatives for 4-nitroaniline using CC2 with a larger basis set are computationally very demanding. However, to check the importance of diffuse functions we have determined $(\partial(\Delta\mu)/\partial Q_k)$ for some of the functionals using the aug-cc-pVTZ basis set. The average unsigned relative error in $\partial(\Delta\mu)/\partial Q_k$ for the cc-pVTZ basis set is presented in Table 3. On average, the extension of the basis set by adding a set of diffuse functions changes the strength of the coupling by not more than 10%. The smallest variations are observed for mode n_1 (2.0%) and the largest for mode n_2 (9.5%). It can thus be concluded that the differences in the results predicted by the two basis sets are not significant. Likewise, an overall satisfactory agreement in IR spectra predicted using cc-pVTZ and aug-cc-pVTZ basis set is found at the CC2 level (results are shown in Supporting Information). Thus, hereafter we will only discuss the properties obtained using the smaller (cc-pVTZ) basis set. Several interesting conclusions can be drawn based on the analysis of Figure 1. Except M06-HF, the strength of the coupling for mode n_1 is predicted by all other used functionals to exceed 4 D/(Å$\sqrt{\text{amu}}$) and the value varies from 4.23 (BHandHLYP) to 4.54 D/(Å$\sqrt{\text{amu}}$) (B3LYP). The value computed at the CC2 level is 3.53 D/(Å$\sqrt{\text{amu}}$) and is

Table 3. Unsigned percentage relative error in $\partial(\Delta\mu)/\partial Q_k$ (k=$n_1,\ldots,n_5$) computed using the cc-pVTZ basis set with respect to the value computed using the aug-cc-pVTZ.

	n_1	n_2	n_3	n_4	n_5
B3LYP	2.3	12.2	0.4	4.1	17.8
BHandHLYP	1.0	9.8	7.9	4.8	9.1
CAM-B3LYP	1.7	7.7	2.8	3.9	1.9
M06	3.1	11.4	10.3	9.8	6.0
PBE0	2.0	6.3	3.6	6.4	1.5
Average error	2.0	9.5	5.0	5.8	7.3

significantly lower than any of the above mentioned functionals. Conversely, M06-HF functional substantially underestimates the coupling and predicts the value for mode n_1 to be only 1.80 D/(Å$\sqrt{\text{amu}}$). Likewise, for any other mode in the range 1100–1800 cm^{-1}, the M06-HF functional underestimates the strength of the coupling $\partial(\Delta\mu)/\partial Q_k$. It is worth recalling that the M06-HF functional predicts the smallest dipole moment change on excitation to the (π,π^*) excited state of 4-nitroaniline (only 4.3 D). Here, we demonstrate that it also performs poorly in predicting changes of $\Delta\mu$ on vibration. For the modes n_2 and n_3 B3LYP, M06, and PBE0 predict much larger strength of the coupling than the CC2 method. For example, the value of $\partial(\Delta\mu)/\partial Q$ for n_3 computed using the B3LYP functional is 3.30 D/(Å$\sqrt{\text{amu}}$) and only 0.98 D/(Å$\sqrt{\text{amu}}$) at the CC2 level of theory. CAM-B3LYP and BHandHLYP functionals predict the strength of the coupling for the modes n_2 and n_3 in much better agreement with the CC2 results. As far as the last two modes in the discussed spectral range are concerned, that is, n_4 and n_5, all methods consistently predict that the coupling strength is larger for mode n_4 than for mode n_5 (note that some methods predict reverse ordering of these modes, cf. Table 2). However, the intensity ratio of the coupling strength (n_4:n_5) varies strongly among used functionals from 1.09 (BHandHLYP) up to 7.88 (M06-HF). B3LYP predicts the value of the ratio to be 1.72 and it is in the best agreement with the CC2 value (1.43). Except the M06-HF functionals which delivers the worst predictions of coupling strengths, the performance of used functionals is somewhat mixed and much depends on the spectral range and type of vibration. Considering the values of $\partial(\Delta\mu)/\partial Q_k$ for all five modes, the best agreement with the CC2 data is observed for CAM-B3LYP and BHandHLYP.

The derivatives of the longitudinal component of two-photon transition moment with respect to normal modes in the range 200–1800 cm^{-1} are shown in Figure 2. As seen, below 1100 cm^{-1} there are some low-frequency modes of

Table 2. Ordering and assignments[51] of normal modes of largest coupling either to $\Delta\mu$ or M^{ZZ}. The values in parentheses correspond to unscaled harmonic vibrational frequencies (given in cm^{-1}) determined using the cc-pVTZ basis set.

	B3LYP	BHandHLYP	CAM-B3LYP	M06	M06-HF	PBE0	CC2
n_1: ν(7*a*,ph-NO_2),ν(ph-1)	24 (1129)	24 (1184)	24 (1150)	24 (1118)	25 (1173)	25 (1145)	24 (1108)
n_2: ν(13,ph-NH_2), ν(ph-12), δ(CH-18a)	27 (1331)	27 (1378)	28 (1349)	28 (1337)	29 (1352)	28 (1350)	29 (1321)
n_3: ν_s(NO_2), ν(ph-NO_2)	29 (1365)	30 (1486)	30 (1429)	30 (1416)	31 (1509)	30 (1422)	27 (1286)
n_4: ν(ph-8a), δ_s(NH_2), δ(CH-9a)	35 (1644)	34 (1712)	36 (1687)	35 (1666)	35 (1691)	35 (1681)	34 (1632)
n_5: δ_s(NH_2-scissoring), ν(ph-8a), δ(CH-9a), ν(ph-NH_2)	36 (1664)	35 (1730)	34 (1662)	34 (1630)	34 (1662)	34 (1653)	36 (1657)

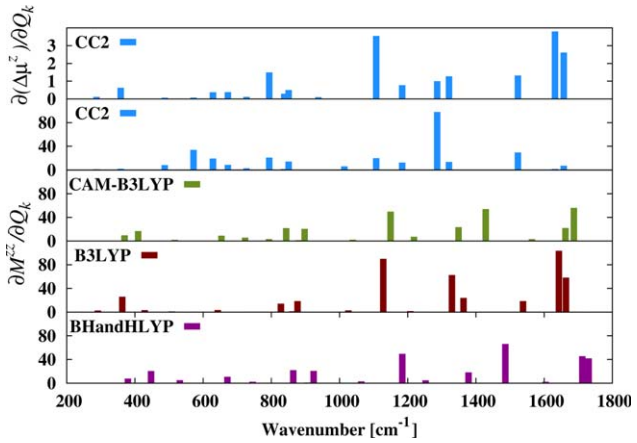


Figure 2. Geometric derivatives of two-photon transition moment corresponding to the transition to the (π,π^*) excited state for 4–nitroaniline *in vacuo*. All values are given in [au/(Å$\sqrt{\text{amu}}$)]. Upper panel presents the geometric derivatives of dipole moment difference between the (π,π^*) excited state and the ground electronic state (given in [Debye/(Å$\sqrt{\text{amu}}$)]). All data were obtained using the cc-pVTZ basis set.

moderate coupling strength. Due to a limited implementation of quadratic response functions at the density functional level, the calculations of geometric derivatives of M^{ZZ} were performed only for three functionals: BHandHLYP, B3LYP, and CAM-B3LYP. The intensity ordering for the five key modes is $n_3 > n_1 > n_2 > n_5 > n_4$ (CC2), $n_4 > n_3 > n_1 > n_2 > n_5$ (CAM-B3LYP), $n_4 > n_1 > n_2 > n_5 > n_3$ (B3LYP) and $n_3 > n_1 > n_4 > n_5 > n_2$ (BHandHLYP). As seen, each method predicts different ordering and yet the amplitudes of the coupling vary strongly. The largest coupling strength at the CC2 level is found for mode n_3 and the corresponding value is 97.8 [au/(Å$\sqrt{\text{amu}}$)]. The density functionals predict much smaller values of the coupling strength for this mode, that is, 53.9 (CAM-B3LYP), 23.9 (B3LYP) and 66.2 [au/(Å$\sqrt{\text{amu}}$)] (BHandHLYP). Conversely, the largest value at the B3LYP level is found for mode n_4 and it equals to 103.4 [au/(Å$\sqrt{\text{amu}}$)]. To sum up, we note large variations in coupling patterns among three used exchange-correlation functionals and none of them resembles that predicted by CC2. Finally, an interesting piece of information emerges from the comparison of $\partial(\Delta\mu^Z)/\partial Q_k$ and $\partial M^{ZZ}/\partial Q_k$ computed using the CC2 method [cf. Fig. 2 (upper two panels)]. Namely, the three modes of largest coupling to $\Delta\mu^Z$ (n_1, n_4, and n_5) only weakly couple to M^{ZZ}. Conversely, as discussed above, it is mode n_3 that exhibits by far the strongest coupling to M^{ZZ}. One may thus draw the conclusion that the approximate representation of geometric derivatives of M^{ZZ} by $\partial(\Delta\mu^Z)/\partial Q_k$ is not universally legitimate, even in the case of the charge-transfer $\pi \rightarrow \pi^*$ transition for the studied prototypical push–pull system.

What we have studied thus far was the assessment of commonly used exchange-correlation functionals for computing the coupling strength of the two-photon transition moment (or $\Delta\mu$) to normal modes of vibration. However, a fine structure of the TPA band is not solely determined by the coupling strength but it does also depend on the matrix elements between vibrational wave functions in the ground and excited states. In this article, we use a linear coupling model to simulate the vibrational fine structure of TPA bands. Thus, we retain terms up to linear in the expansion of the two-photon transition moment with respect to the normal coordinate. The results of simulations of TPA spectra for each method used to determine the geometric derivatives of M^{ZZ} are presented in Figure 3. As we consider 4-nitroaniline *in vacuo*, we simulated the spectra assuming only a homogeneous broadening represented by Lorentzian profile. To conveniently compare all used electronic structure methods, the spectra presented in Figure 3 are normalized (with respect to the most intense feature at the B3LYP level) and the 0-0 transition for all methods is located at 0 cm^{-1}. First, we note that there are substantial differences in the total TPA intensity distribution between B3LYP and the remaining methods. CAM-B3LYP and BHandHLYP yield very similar profiles that are qualitatively similar to that predicted by CC2. The decomposition of the total intensity into FC, HT and mixed FC/HT terms show, in agreement with the results obtained by Silverstein and Jensen using LC-PBE functional,[13] that the TPA profile for 4-nitroaniline is largely determined by the FC contribution. However, the CC2 results bring new insight into the vibronic coupling mechanism in TPA spectra of 4-nitroniline and demonstrate that the mixed term is quite large and that it also exhibits the negative interference with the FC contribution. It should be noted that the importance of non-Condon effects in TPA spectra has already been reported, including some of the present authors.[24,25,52] This study clearly demonstrates that the conclusions might strongly depend on the used electronic structure method. The discrepancies in band structure might be attributed to the differences in Huang–Rhys factors (related to the normal mode displacements between the ground and excited state).[53] To put the differences in the displacements on quantitative basis, we have determined the vibrational reorganization energy defined as $\lambda_v = \sum_k(\omega_k\Delta_k^2/2)$, where Δ_k is a dimensionless normal mode displacement for mode k and the index runs over normal modes. The values of λ_v computed at B3LYP, BHandHLYP, CAM-B3LYP, and CC2 levels are 1253, 2323, 2212, and 3664 cm^{-1}, respectively. As seen, B3LYP underestimates substantially the vibrational reorganization energy, while BHandHLYP and CAM-B3LYP yield similar values of λ_v. This explains the very similar FC profiles predicted by the two functionals. Conversely, CC2 predicts a much larger value than the other functionals. The difficulties in estimation of vibrational reorganization energy for 4-nitroaniline using the B3LYP functional have already been discussed by Silverstein and Jensen.[13] These authors determined the value of λ_v at the B3LYP/cc-pVDZ level to be 863 cm^{-1}. The latter value, apart from differences in the basis set used, cannot be directly compared to present result due to the fact that Silverstein and Jensen studied a nonequilibrium C_{2v} structure of 4-nitroaniline. Nevertheless, these authors also reported that the LC-PBE functional predicts a much larger value of λ_v, that is in agreement with the present findings.

It is relevant to mention that Moran and Kelley determined experimentally dimensionless normal mode displacements for

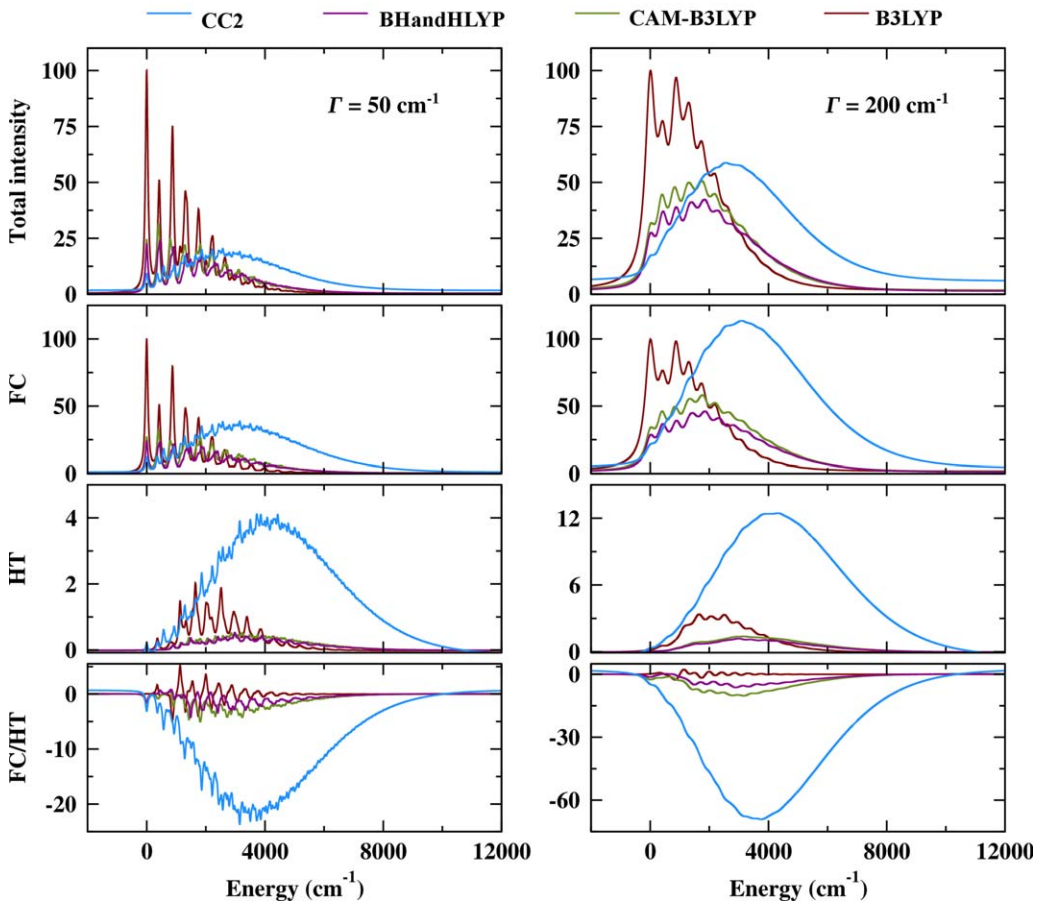


Figure 3. Vibronic TPA spectra for 4–nitroaniline *in vacuo* simulated based on the dominant longitudinal component of two-photon transition moment. All data were obtained using the cc-pVTZ basis set.

several modes in five solvents.[54] Our gas-phase results can be compared with the experimental data obtained for cyclehexane, which is a low-polarity solvent. The value of λ_v computed at the CC2 level for the 5 modes reported by Moran and Kelley is 2045 cm^{-1} and is in reasonable agreement with the experimental data (2058 cm^{-1}). Although the method used by Moran and Kelley to determine dimensionless mode displacements has its limitations,[48] it gives strong support for CC2 as the reference level for the present study. Moreover, to quantify the differences in TPA profiles computed at several levels of approximation, we introduce β parameter defined as:

$$\beta = \left[\frac{\int [I_{tot}^{CC2}(v) - I_{tot}^{DFT}(v)]^2 dv}{\int [I_{tot}^{CC2}(v)]^2 dv}\right]^{\frac{1}{2}} \quad (3)$$

By definition, $\beta = 0$ for identical spectral profiles. We have determined this parameter for all used functionals (B3LYP, CAM-B3LYP, BHandHLYP) with respect to the CC2 profile for total vibronic 2PA spectra (FC+FC/HT+HT) with broadening equal to 200 cm^{-1}. The value of β is 0.990, 0.602, and 0.613 for B3LYP, CAM-B3LYP, and BHandHLYP functional, respectively. These numbers demonstrate that both CAM-B3LYP and BHandHLYP yield similar absorption profiles and they are in line with the visual inspection of Figure 3. Conversely, the β value computed for the B3LYP spectrum is roughly 30% larger than that obtained for two other functionals.

Summary

In this study, we performed computations of vibrational fine structure of TPA band for 4-nitroaniline *in vacuo*. Vibronic TPA spectra were simulated within the framework of the linear coupling model and using resolution-of-identity implementation of the approximate second-order coupled-cluster singles and doubles model CC2 with the cc-pVTZ basis set. The CC2 results bring new insight into the vibronic coupling mechanism in TPA spectra of 4-nitroniline and demonstrate that the mixed term is quite large and that it also exhibits a negative interference with the FC contribution. A substantial part of this study was devoted to the comparative assessment of several popular exchange-correlation functionals in simulations of vibronic TPA spectrum as well as in computing geometric derivatives of the two-photon transition moment and the dipole moment difference for the charge-transfer state. This study demonstrates that there are large variations in the coupling strength of two-photon transition moments to normal coordinates for the used set of functionals. None of the exchange-correlation functionals predicts the coupling pattern similar to that computed at the CC2 level for the key normal

modes, that is, modes characterized by the largest values of $\partial M/\partial Q$. These differences, however, have only a secondary effect on the simulated TPA spectra of 4-nitroaniline in gas phase. The shape of the TPA band profile, largely dominated by the Franck–Condon contribution, crucially depends on the normal mode displacements. An attempt to quantify the differences in vibronic TPA profiles reveals that BHandHLYP or CAM-B3LYP functionals outperforms B3LYP functional. Nevertheless, in comparison with CC2 spectrum, none of the studied functionals satisfactorily predicts vibronic profiles for 4-nitroaniline.

Acknowledgments

R.Z. is a Wenner-Gren Foundations scholar. Part of calculations was performed at Academic Computer Centre CYFRONET AGH.

Keywords: two-photon absorption · density functional theory · CC2 method · vibronic coupling · range-separated hybrid functionals · excited states

How to cite this article: R., Zaleśny, G. Tian, C. Hättig, W. Bartkowiak, H. Ågren. *J. Comput. Chem.* **2015**, *36*, 1124–1131. DOI: 10.1002/jcc.23903

Additional Supporting Information may be found in the online version of this article.

[1] B. Champagne, E. A. Perpète, S. J. A. van Gisbergen, E. J. Baerends, J. G. Snijders, C. Soubra-Ghaoui, K. A. Robins, B. Kirtman, *J. Chem. Phys.* **1998**, *109*, 10489.
[2] B. Champagne, E. A. Perpète, D. Jacquemin, S. J. A. van Gisbergen, E. J. Baerends, C. Soubra-Ghaoui, K. A. Robins, B. Kirtman, *J. Phys. Chem. A* **2000**, *104*, 4755.
[3] S. J. A. van Gisbergen, P. R. T. Schipper, O. V. Gritsenko, E. J. Baerends, J. G. Snijders, B. Champagne, B. Kirtman, *Phys. Rev. Lett.* **1999**, *83*, 694.
[4] J. R. Hammond, K. Kowalski, *J. Chem. Phys.* **2009**, *130*, 194108.
[5] P. A. Limacher, K. V. Mikkelsen, H. P. Lüthi, *J. Chem. Phys.* **2009**, *130*, 194114.
[6] S.-I. Lu, *Theor. Chem. Acc.* **2013**, *133*, 1439.
[7] S.-I. Lu, C.-C. Chiu, Y.-F. Wang, *J. Chem. Phys.* **2011**, *135*, 134104.
[8] A. Baranowska-Łączkowska, W. Bartkowiak, R. W. Góra, F. Pawłowski, R. Zaleśny, *J. Comput. Chem.* **2013**, *34*, 819.
[9] D. Jacquemin, E. A. Perpète, M. Medved, G. Scalmani, M. J. Frisch, R. Kobayashi, C. Adamo, *J. Chem. Phys.* **2007**, *126*, 191108.
[10] S. Nénon, B. Champagne, M. I. Spassova, *Phys. Chem. Chem. Phys.* **2014**, *16*, 7083.
[11] K. Garrett, X. Sosa Vazquez, S. B. Egri, J. Wilmer, L. E. Johnson, B. H. Robinson, C. M. Isborn, *J. Chem. Theory Comput.* **2014**, *0*, null.
[12] D. L. Silva, N. A. Murugan, J. Kongsted, Z. Rinkevicius, S. Canuto, H. Ågren, *J. Phys. Chem. B* **2012**, *116*, 8169.
[13] D. W. Silverstein, L. Jensen, *J. Chem. Phys.* **2012**, *136*, 064110.
[14] D. H. Friese, C. Hattig, K. Ruud, *Phys. Chem. Chem. Phys.* **2012**, *14*, 1175.
[15] N. A. Murugan, R. Zaleśny, J. Kongsted, H. Ågren, *J. Chem. Theory Comput.* **2014**, *10*, 778.
[16] M. Wielgus, R. Zaleśy, N. A. Murugan, J. Kongsted, H. Ågren, M. Samoc, W. Bartkowiak, *ChemPhysChem* **2013**, *14*, 3731.
[17] J. Olesiak-Banska, K. Matczyszyn, R. Zaleśny, N. A. Murugan, J. Kongsted, H. Ågren, W. Bartkowiak, M. Samoc, *J. Phys. Chem. B* **2013**, *117*, 12013.
[18] R. Zaleśny, I. W. Bulik, W. Bartkowiak, J. M. Luis, A. Avramopoulos, M. G. Papadopoulos, P. Krawczyk, *J. Chem. Phys.* **2010**, *133*, 244308.
[19] I. W. Bulik, R. Zaleśny, W. Bartkowiak, J. M. Luis, B. Kirtman, G. E. Scuseria, A. Avramopoulos, H. Reis, M. G. Papadopoulos, *J. Comput. Chem.* **2013**, *34*, 1775.
[20] P. Macak, Y. Luo, P. Norman, H. Ågren, *J. Chem. Phys.* **2000**, *113*, 7055.
[21] P. Macak, Y. Luo, H. Ågren, *Chem. Phys. Lett.* **2000**, *330*, 447.
[22] D. M. Bishop, J. M. Luis, B. Kirtman, *J. Chem. Phys.* **2002**, *116*, 9729.
[23] D. W. Silverstein, L. Jensen, *J. Chem. Phys.* **2012**, *136*, 064111.
[24] M. Drobizhev, N. S. Makarov, S. E. Tillo, T. E. Hughes, A. Rebane, *J. Phys. Chem. B* **2012**, *116*, 1736.
[25] Y. Ai, G. Tian, Y. Luo, *Mol. Phys.* **2013**, *111*, 1316.
[26] O. Christiansen, H. Koch, P. Jørgensen, *Chem. Phys. Lett.* **1995**, *243*, 409.
[27] H. Koch, P. Jørgensen, *J. Chem. Phys.* **1990**, *93*, 3333.
[28] C. Hättig, O. Christiansen, P. Jørgensen, *J. Chem. Phys.* **1998**, *108*, 8331.
[29] M. Medved, M. Stachová, D. Jacquemin, J.-M. André, E. A. Perpète, *J. Mol. Struct. (THEOCHEM)* **2007**, *847*, 39.
[30] T. H. Dunning, *J. Chem. Phys.* **1989**, *90*, 1007.
[31] R. A. Kendall, T. H. Dunning, R. J. Harrison, *J. Chem. Phys.* **1992**, *96*, 6796.
[32] D. E. Woon, T. H. Dunning, *J. Chem. Phys.* **1994**, *100*, 2975.
[33] T. Yanai, D. P. Tew, N. C. Handy, *Chem. Phys. Lett.* **2004**, *393*, 51.
[34] P. J. Stephens, F. J. Devlin, C. F. Chabalowski, M. J. Frish, *J. Phys. Chem.* **1994**, *98*, 11623.
[35] M. J. Frisch, G. W. Trucks, H. B. Schlegel, G. E. Scuseria, M. A. Robb, J. R. Cheeseman, G. Scalmani, V. Barone, B. Mennucci, G. A. Petersson, H. Nakatsuji, M. Caricato, X. Li, H. P. Hratchian, A. F. Izmaylov, J. Bloino, G. Zheng, J. L. Sonnenberg, M. Hada, M. Ehara, K. Toyota, R. Fukuda, J. Hasegawa, M. Ishida, T. Nakajima, Y. Honda, O. Kitao, H. Nakai, T. Vreven, J. A. Montgomery, Jr., J. E. Peralta, F. Ogliaro, M. Bearpark, J. J. Heyd, E. Brothers, K. N. Kudin, V. N. Staroverov, R. Kobayashi, J. Normand, K. Raghavachari, A. Rendell, J. C. Burant, S. S. Iyengar, J. Tomasi, M. Cossi, N. Rega, J. M. Millam, M. Klene, J. E. Knox, J. B. Cross, V. Bakken, C. Adamo, J. Jaramillo, R. Gomperts, R. E. Stratmann, O. Yazyev, A. J. Austin, R. Cammi, C. Pomelli, J. W. Ochterski, R. L. Martin, K. Morokuma, V. G. Zakrzewski, G. A. Voth, P. Salvador, J. J. Dannenberg, S. Dapprich, A. D. Daniels, Ö. Farkas, J. B. Foresman, J. V. Ortiz, J. Cioslowski, D. J. Fox, GAUSSIAN 09 Revision D.01, Gaussian Inc.: Wallingford CT, **2009**.
[36] Y. Zhao, N. E. Schultz, D. G. Truhlar, *J. Chem. Theory Comput.* **2006**, *2*, 364.
[37] Y. Zhao, N. E. Schultz, D. G. Truhlar, *J. Chem. Phys.* **2005**, *123*, 161103.
[38] M. Ernzerhof, G. E. Scuseria, *J. Chem. Phys* **1999**, *110*, 5029.
[39] C. Adamo, V. Barone, *J. Chem. Phys.* **1999**, *110*, 6158.
[40] H. Iikura, T. Tsuneda, T. Yanai, K. Hirao, *J. Chem. Phys.* **2001**, *115*, 3540.
[41] J.-D. Chai, M. Head-Gordon, *J. Chem. Phys.* **2008**, *128*, 084106.
[42] K. Aidas, C. Angeli, K. L. Bak, V. Bakken, R. Bast, L. Boman, O. Christiansen, R. Cimiraglia, S. Coriani, P. Dahle, E. K. Dalskov, U. Ekstrom, T. Enevoldsen, J. J. Eriksen, P. Ettenhuber, B. Fernandez, L. Ferrighi, H. Fliegl, L. Frediani, K. Hald, A. Halkier, C. Hattig, H. Heiberg, T. Helgaker, A. C. Hennum, H. Hettema, E. Hjertenas, S. Host, I.-M. Hayvik, M. F. Iozzi, B. Jansik, H. J. A. Jensen, D. Jonsson, P. Jorgensen, J. Kauczor, S. Kirpekar, T. Kjergaard, W. Klopper, S. Knecht, R. Kobayashi, H. Koch, J. Kongsted, A. Krapp, K. Kristensen, A. Ligabue, O. B. Lutnis, J. I. Melo, K. V. Mikkelsen, R. H. Myhre, C. Neiss, C. B. Nielsen, P. Norman, J. Olsen, J. M. H. Olsen, A. Osted, M. J. Packer, F. Pawlowski, T. B. Pedersen, P. F. Provasi, S. Reine, Z. Rinkevicius, T. A. Ruden, K. Ruud, V. V. Rybkin, P. Salek, C. C. M. Samson, A. S. de Meras, T. Saue, S. P. A. Sauer, B. Schimmelpfennig, K. Sneskov, A. H. Steindal, K. O. Sylvester-Hvid, P. R. Taylor, A. M. Teale, E. I. Tellgren, D. P. Tew, A. J. Thorvaldsen, L. Thogersen, O. Vahtras, M. A. Watson, D. J. D. Wilson, M. Ziolkowski, H. Ågren, *WIREs Comput. Mol. Sci.* **2014**, *4*, 269.
[43] TURBOMOLE V6.4 2012, a development of University of Karlsruhe, Forschungszentrum Karlsruhe GmbH, 1989–2007, TURBOMOLE GmbH, since 2007; Available from: http://www.turbomole.com.
[44] F. Furche, R. Ahlrichs, C. Hattig, W. Klopper, M. Sierka, F. Weigend, *WIREs Comput. Mol. Sci.* **2014**, *4*, 91.
[45] C. Hättig, F. Weigend, *J. Chem. Phys.* **2000**, *113*, 5154.
[46] F. Weigend, A. Köhn, C. Hättig, *J. Chem. Phys.* **2002**, *116*, 3175.
[47] J. Bednarska, A. Roztoczyńska, W. Bartkowiak, R. Zaleśny, *Chem. Phys. Lett.* **2013**, *584*, 58.

[48] G. Scalmani, M. J. Frisch, B. Mennucci, J. Tomasi, R. Cammi, V. Barone, *J. Chem. Phys.* **2006**, *124*, 094107.
[49] C. Hättig, A. Köhn, *J. Chem. Phys.* **2002**, *117*, 6939.
[50] J. J. Eriksen, S. P. A. Sauer, K. V. Mikkelsen, O. Christiansen, H. J. A. Jensen, J. Kongsted, *Mol. Phys.* **2013**, *111*, 1235.
[51] V. Kozich, W. Werncke, J. Dreyer, K. W. Brzezinka, M. Rini, A. Kummrow, T. Elsaesser, *J. Chem. Phys.* **2002**, *117*, 719.
[52] E. Kamarchik, A. I. Krylov, *J. Phys. Chem. Lett.* **2011**, *2*, 488.
[53] K. Huang, A. Rhys, Proc. R. *Soc. London, Ser. A* **1950**, *204*, 406.
[54] A. M. Moran, A. M. Kelley, *J. Chem. Phys.* **2001**, *115*, 912.

Received: 30 October 2014
Revised: 24 February 2015
Accepted: 28 February 2015
Published online on 31 March 2015